Journal of Materials Chemistry A

Accepted Manuscript

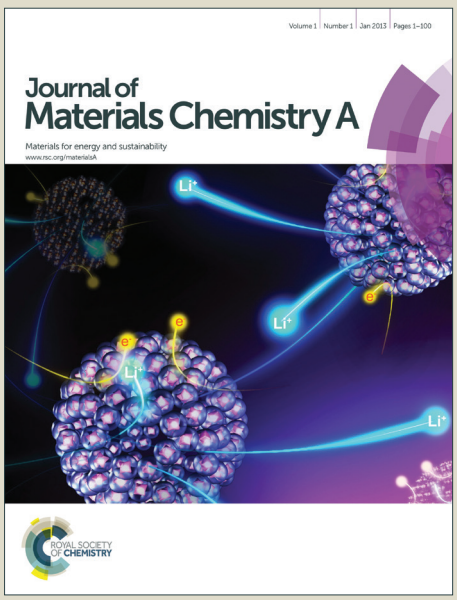

ROYAL SOCIETY OF CHEMISTRY

www.rsc.org/materialsA

Journal Name

RSCPublishing

ARTICLE

Sustainable production of HCOOH via an electrolytic reduction of gas-phase $^{12}CO_2$

Cite this: DOI: 10.1039/x0xx00000x

Seunghwa Lee,[a] HyungKuk Ju,[b] Revocatus Machunda,[b] Sunghyun Uhm,[bc] Jae Kwang Lee,[b] Hye Jin Lee,[d] and Jaeyoung Lee[*ab]

Received 00th January 2012,
Accepted 00th January 2012

DOI: 10.1039/x0xx00000x

www.rsc.org/

A tin (Sn) nanostructure onto gas diffusion electrode is applied for the direct electroreduction of carbon dioxide (CO_2) in a zero-gap electrolytic cell. Sn catalyst layer is evenly placed onto carbon substrates by a controlled spraying procedure and its efficient catalytic conversion of gas-phased CO_2 to formic acid (HCOOH) is demonstrated. We observe that the overall mean faradaic efficiency towards HCOOH stays over 5.0% during the entire reduction time. Furthermore, note that the approach employed in this study is promising for modularity and scalability due to its compact configuration and surroundings under near ambient conditions. Sustainable energy sources such as solar, wind, and geothermal electricity could be used as a continuous power source in order to decrease the overall cost for CO_2 utilization..

Introduction

In the 21st century our world is still searching for strategies to overcome the challenges associated with climate change, dependency on fossil fuels and limited natural resources. Solar energy is trapped in the atmosphere as heat by several gases including typically carbon dioxide (CO_2), methane (CH_4) and chlorofluorocarbon (CFCs). The so-called greenhouse effect is now widely accepted as a significant environmental threat. Supplies of fossil fuels and natural gases are dwindling and this has propelled a search for potential renewable and alternative energy supply.

Technologies to curtail greenhouse gas emissions especially CO_2 have been carried out through a variety of methods.[1,2] Currently, carbon capture and storage (CCS) has received considerable attentions as one of the technologies to handle large quantities of CO_2 emissions.[1-3] Sequestration has been the major storage option for CO_2 gas from power plants, but several shortcomings remain, including environmental and safety concerns about the risk of leakage as well as technological limitations.[3]

Considerable efforts have been made on heterogeneous catalysis for the conversion of CO_2 gas into value-added chemicals as an alternative long-term solution for the CO_2 mitigation.[2,4] The utilisation of CO_2 gas is limited by the fact that it requires significant activation energy for transformation into organic chemicals thus a superior catalyst must be used to overcome the high activation energy barrier. Hence, the reduction process for selecting products necessitates the use of specific metal catalysts.[5] Azuma et al. summarized the types of catalysts within the periodic table showing product distributions in specific condition and Hori et al. divided them into four types of catalysts.[6,7]

Effective conversion will thus require the use of good catalysts and systems which can convert large volumes using low cost reactants available. In general, electrocatalysts are categorized into *sp* metals (Zn, Cd, Hg, In, Tl, Pb, Ti and Sn) for HCOOH and *d* metals (Pd, Pt, Cu, Ag and Au) for CO according to the electronic configuration related to their electrocatalytic behavior.[8] Among these metals, we investigated

[a] Electrochemical Reaction and Technology Laboratory, School of Environmental Science and Engineering, Gwangju Institute of Science and Technology (GIST), Gwangju, 500-712, South Korea. E-mail: jaeyoung@gist.ac.kr

[b] Ertl Center for Electrochemistry and Catalysis, Research Institute for Solar and Sustainable Energies, GIST, Gwangju, 500-712, South Korea.

[c] Advanced Materials and Processing Center, Institute for Advanced Engineering (IAE), Gyeonggi-do, 449-863, South Korea.

[d] Department of Chemistry and Green-Nano Materials Research Center, Kyungpook National University, Daegu, 702-701, South Korea.

† Electronic Supplementary Information (ESI) available: [details of any supplementary information available should be included here]. See DOI: 10.1039/b000000x/

Sn electrocatalyst for the selective production of HCOOH since Sn is inexpensive and relatively less toxic compared to other metals. A new approach using zero-gap cell with GDE was first introduced for the effective electrocatalytic reduction of gas-phase CO_2, while alleviating mass-transfer limitations caused by the low solubility of CO_2 in liquid phase systems.

The direct production of small organic molecules from CO_2 is still far from feasibility and the large scale production is even more challenging. Of the small organic molecules, HCOOH produced from the reduction process have higher value from the energy required for their production, because of its significant uses in various areas such as fuels in fuel cells, fertilizers, pharmaceuticals in addition to feedstocks for various chemical industries, than other organic products such as methanol (CH_3OH), ethylene (C_2H_4) and methane (CH_4).[9] The main mechanism of the electroreduction of CO_2 taking place at the cathode is given by the following equations.[10]

$$CO_{2(g)} \rightarrow CO_{2(ad)} \quad (1)$$

$$CO_{2(ad)} + e^- \rightarrow \cdot {CO_2}^-_{(ad)} \quad (2)$$

$$\cdot {CO_2}^-_{(ad)} + H^+ \rightarrow \cdot HCOO_{(ad)} \quad (3)$$

$$\cdot HCOO_{(ad)} + e^- \rightarrow \cdot HCOO^-_{(aq)} \quad (4)$$

$$\cdot HCOO^-_{(aq)} + H^+ \rightarrow HCOOH \quad (5)$$

The overall reaction of the formation of HCOOH is:

$$CO_{2(g)} + 2H^+ + 2e^- \rightarrow HCOOH \quad (6)$$

The catalytic activity of gaseous CO_2 into the intended product, HCOOH, could be reported by both the product yield and faradaic efficiency.[11] Therefore, improving the efficiency of this conversion will result in the scale-up of the system and stabilization of CO_2 gas emissions. Preti et al. reported a faradaic efficiency of ca. 83% to produce HCOOH from CO_2 under the high pressure of 180 bar and Yan et al. showed a yield of 87% of HCOOH over about 300°C.[12,13]

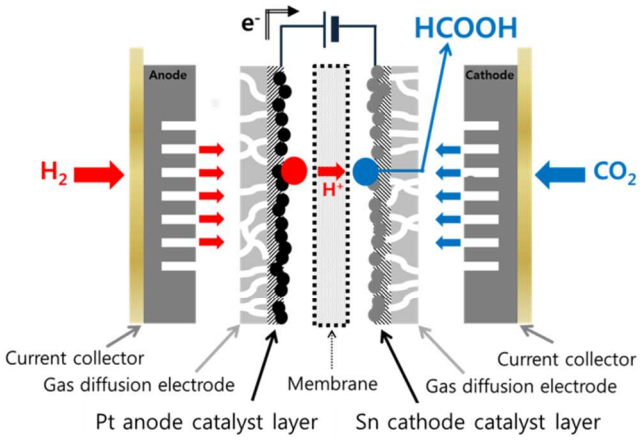

Figure 1. Schematic diagram of a zero gap electrolytic cell configuration for the electroreduction of CO2 supplied directly from gas phase.

However, both studies required high temperatures and pressures. Our previous work performed under mild ambient conditions showed that the electro-deposition of Sn did not provide a sufficient loading and a homogeneous coating on the entire electrode surface.[14] As a result, a low and unstable product yield was obtained. In this work, we describe a novel method to homogeneously coat a thin layer of Sn nanopowders on gas diffusion electrode (Figure 1) by a controlled spraying method and demonstrate the better performance than that of the previous work in terms of activity and long-term stability.

Results and discussion

Identification of gas-phase CO_2 electroreduction

A fundamental and immediate question arises as to whether the carbon converted to HCOOH originated from CO_2 gas or not, since the corrosion of the carbon electrode is known to occur under the high overvoltage applied.[15] Hence, our first investigation was focused on verifying the conversion of gas-phase CO_2 into the liquid form of HCOOH.

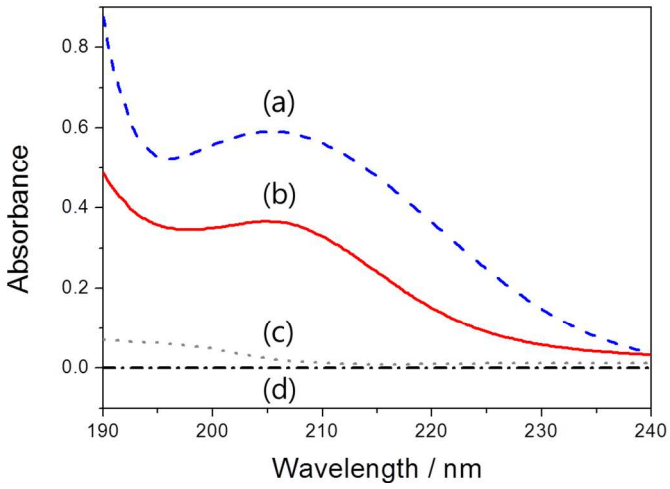

Figure 2. UV-spectroscopy analysis of the produced HCOOH to compare experiments performed under different conditions : (a) commercial HCOOH for standard reference, (b) electroreduction of gaseous CO_2, (c) electroreduction of inert gas Ar and (d) baseline of deionized water.

Several liquid samples generated under various conditions were analyzed to reveal the carbon source of produced HCOOH by UV-spectroscopy in the wavelength region of 190-240 nm (Figure 2). Deionized water was used as a reference and the maximum absorbance peak at 207 nm from commercial HCOOH solution was matched with each resultant graph of samples. In the absence of CO_2 gas supplied, no peaks corresponding to the HCOOH were observed. In addition, ^{1}H-NMR analysis was performed for the identification of the carbon source more meticulously.[16,17]

In order to trace the carbon source of HCOOH product, $^{13}CO_2$ gas was supplied and converted into the liquid phase

product by the electrochemical reduction process. Carbon isotopes having mass number of 13 u are naturally occurring at as small proportion as about 2%. By intended formation of ^{13}C-labeled HCOOH, the intensities of two types of HCOOH peaks in ^{1}H-NMR spectra were reversed compared to that of the commercial ^{12}C-HCOOH peaks. As shown in Figure 3, it was observed that ^{13}C-labeled HCOOH peaks increased sharply and this result allowed the identification of the carbon source of HCOOH, which was generated from the directly supplied CO_2 gas.

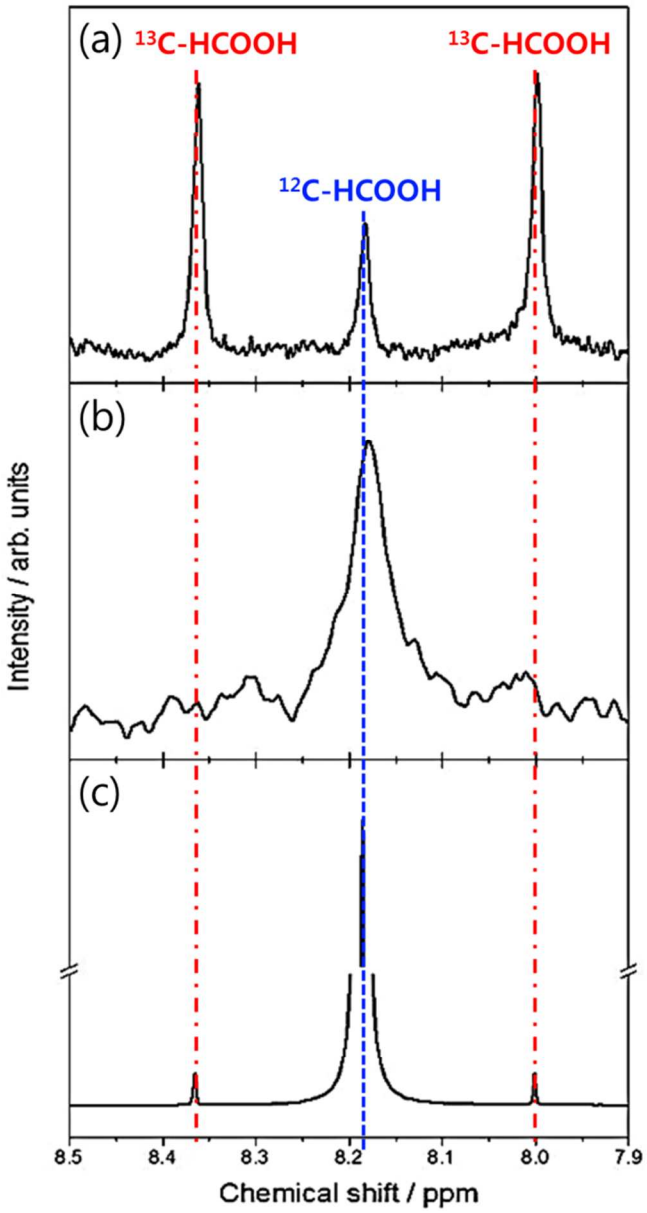

Figure 3. A series of ^{1}H-NMR spectra for HCOOH generated by electrochemical reduction with (a) isotopic $^{13}CO_2$ gas, (b) $^{12}CO_2$ gas and (c) commercial ^{12}C-HCOOH as a reference.

LSV and Optimization of operating conditions

After confirming the origin of carbon converted to HCOOH, the following step was to determine the optimal operating conditions of an electrolytic CO_2 reduction system. Knowing how much Sn catalyst is activated at a given potential is important in the optimization of the system operating conditions. To examine the Sn catalyst's activity for the electroreduction of CO_2, LSV curves were obtained in a zero-gap cell applying both Ar and CO_2. As shown in Figure 4, the voltammogram under CO_2 supplied condition was recorded more negative than that of using the same catalyst under Ar supplied at the cathodic sweep rate of 20 mV sec^{-1}.

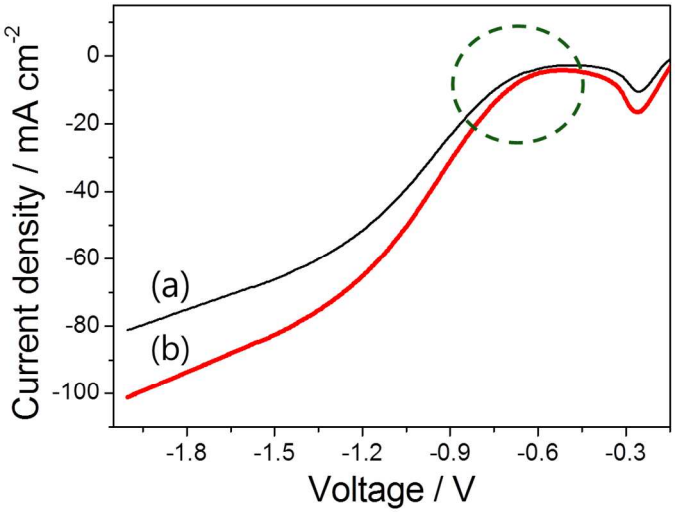

Figure 4. Linear sweep voltammograms using Sn in (a) Ar and (b) CO_2 gas supplied respectively. The reduction peak at -0.7 V was attributed to the electroreduction of CO_2 and another peak appeared at the less negative potential was associated with the hydrogen adsorption. Scan rate was 20 mV sec^{-1}.

We believe that the higher negative current value observed at the cathode voltage around -0.7 V (vs. RHE) was in accordance with CO_2 reduction.

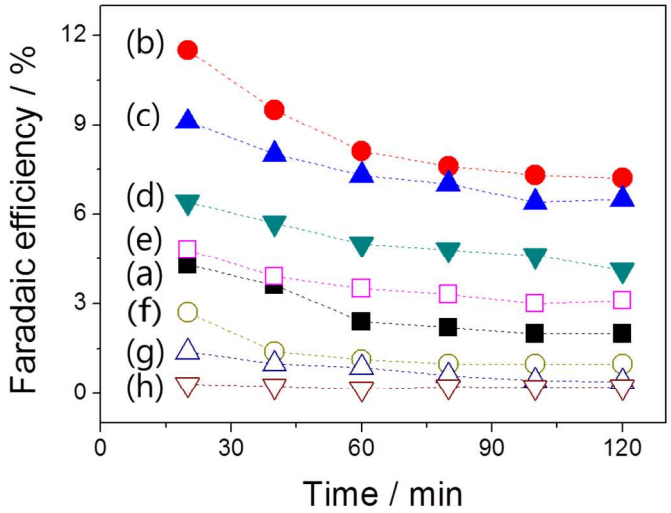

Figure 5. Faradaic efficiencies depending on the various voltages : (a) -0.5 V, (b) -0.7 V, (c) -0.9 V, (d) -1.2 V, (e) -1.4 V, (f) -1.6 V, (g) -1.8 V and (h) -2.0 V.

Based on the observation, the optimal voltage was investigated through experiments while keeping the same conditions of temperature, and gas flow rate (Figure 5).

To suppress the hydrogen production process, the operating temperature was set at room temperature and the gas flow rate of both the anode and cathode were kept at the minimum required to prevent mass transfer limitations (Figure S1).[18,19]

Long-term test for gas-phase CO_2 elecroreduction

Under the optimal conditions based on the above experimental results, the electrochemical reduction of gas-phased CO_2 was carried out at -0.7 V in 10 h of operation. Liquid phase product was collected and analyzed at every 20 min. The variation in currents and faradaic efficiencies in terms of the electrolysis time was evaluated and the measurement outcome is summarized in Figure 6. Sn electrode exhibited the stable current density of 5 mA cm^{-2}. The initial faradaic efficiency towards HCOOH, an average of 12.5%, decreased to about 7% after 3 h running and maintained this level for further few hours until the end of the experiment. The accumulated amount of HCOOH was calculated and the production rate was slightly declined during the electrolytic process (inset of Figure 6).

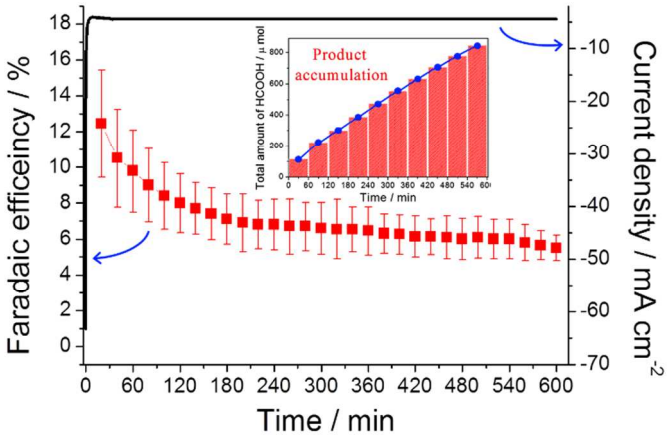

Figure 6. Electrocatalytic activity for the electroreduction of CO_2 on Sn was evaluated by analyzing the production rate of HCOOH vs. time and the current density vs. time at the cathode potential of -0.7 V. Inset image shows the accumulated amount of HCOOH generated from CO_2 electrolysis stably for 10 h.

From the products analysis, the remainder of faradaic current for CO_2 reduction was allotted for the formation of hydrogen (H_2). Decreasing CO_2 reduction performance is attributed to several reasons such as the loss of the sprayed catalyst particles on the GDE, the competitive hydrogen evolution reaction (HER) and the deactivation of the catalyst due to the exposure to concentrated CO_2 gas.[13-15,20]

Morphological investigations of electrode surface

Used electrodes were further analyzed by examining any visual changes in Sn electrocatalyst morphology since the reactivity varied during CO_2 electroreduction. The fabricated electrode was characterized using FE-SEM to reveal the compactness and the uniformity of surface morphology before and after the electrolytic process. Uniformly nanostructured Sn particles were observed on GDE before experiments but the amount of Sn particles decreased after the electrocatalytic reduction of CO_2 (Figure 7). As illustrated in Figure 7b, particle loss was observed indicating that the decomposition of Sn particles could lead to degradation in long term performance.

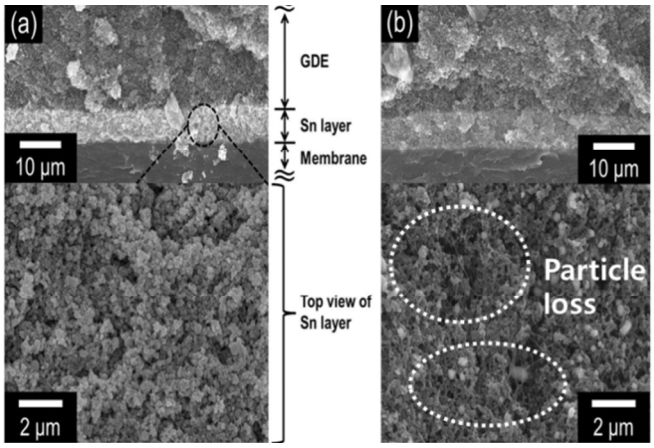

Figure 7. SEM images showing the top-view and cross-section of Sn nanostructured cathode with GDE. (a) As prepared and (b) after the electroreduction of CO_2. Particle loss occurred during CO_2 electrolysis..

Table 1 (Supplementary information) shows the weight of three samples of Sn electrode used in CO2 electroreduction for 1 h, 2 h and 5 h respectively. From the measurement, it is expected that Sn catalyst layer could remain and catalyse the CO2 electroreduction for over 10 h because total weight of Sn catalysts placed on the carbon substrate was 31.5 mg. During CO2 electrolysis of 1 h, decrease of the amount of Sn nanoparticles was almost 2.3 mg and with respect to the electrolytic process time, the particle loss in weight was diminishing gradually similar to the trend of Faradaic efficiency toward HCOOH. Hence, considering result of the long-term electrolysis as seen in Figure 6, the relative weak adhesion between Sn nanoparticles and carbon electrode surface seemed to be functioned as a degradation factor.

In addition, changes in crystallinity during the electrocataysis were examined by XRD. As shown in Figure 8, the electroreduction of CO_2 did not cause any significant changes in crystallinity.

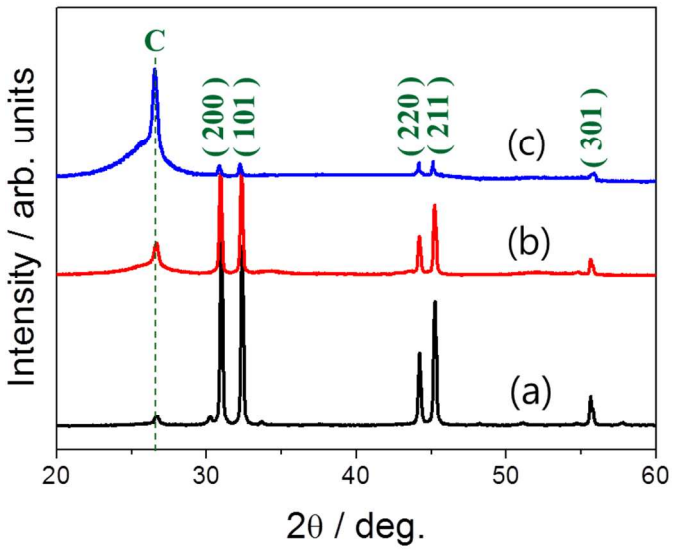

Figure 8. XRD patterns of (a) as-prepared Sn electrode and after electrochemical CO_2 reduction in a zero-gap cell for (b) 3 h and (c) 10 h, respectively

The intensities of Sn peaks decreased due to the loss of catalyst particles from the electrode surface. The increment in the carbon substrate peak also confirms that the catalyst was peeled off from the support material. Consequently, the damage of catalyst configuration on GDE was one of the main contributors to the degradation of the CO_2 electrolysis.[13,14,20]

Moreover, the CO_2 reduction interface was significantly acidified because of sufficient protons from the anode part.[21] It was demonstrated that H_2 was the dominant species from the product analysis in the cathode part. This undesirable reaction pathway could be responsible for the decrease in HCOOH production. In other words, the rate determining step (RDS) is not the transportation of proton and the mass transfer limitation problem of CO_2 was also compensated by directly supplying CO_2 gas to the catalyst onto GDE in a zero gap cell system.

Investigation of RDS by Tafel slope

With these recognitions, Tafel plot was extracted by the same process of CO_2 reduction to investigate the mechanistic pathway regarding RDS. Liquid products were sampled every 20 min and partial current densities for HCOOH production were calculated from faradaic efficiencies. Electrochemical performances for Tafel plot were measured within the window overvoltage ranging from 0.4 to 0.8 V. Tafel law for multi steps reaction is given by:

$$\eta = 2.3\left(\frac{1}{\alpha_c f}\right) logi_0 - 2.3\left(\frac{1}{\alpha_c f}\right) logi \qquad (7)$$

where i_o is the exchange current density expressed in mA cm^{-2}, i is the electrode current density expressed in mA cm^{-2}, α is the transfer coefficient with dimensionless unit, η is the overvoltage expressed in V, f is the RT/F expressed in V^{-1}. The graph of η vs. log i is known as Tafel plot as shown in Figure 9.

If RDS is the formation of CO_2 radical anion (Equation 2), the Tafel slope is theoretically 118 mV dec^{-1}. We obtained the Tafel slope of 148 mV dec^{-1} on Sn electrocatalyst.

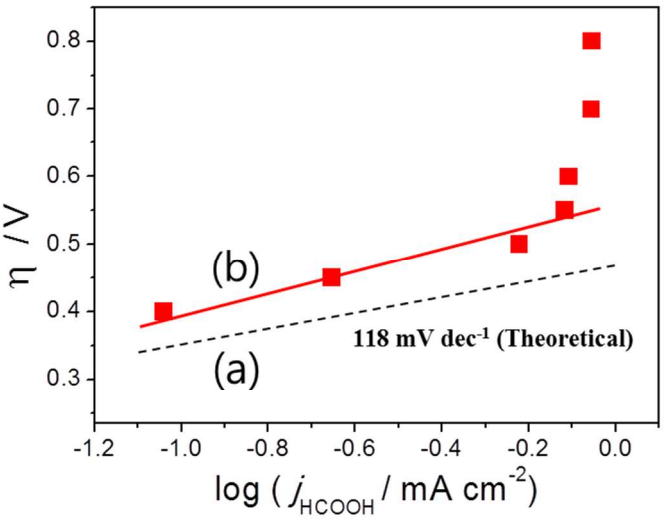

Figure 9. Tafel plot of partial current densities for HCOOH by electroreduction of CO_2. Theoretical Tafel slope of (a) 118 mV dec^{-1} is compared with the Sn electrocatalyst slope of (b) 148 mV dec^{-1} indicating the formation of CO_2 radical anion as RDS.

Tafel slopes of CO_2 reduction for determining the reaction mechanism have previously been studied by many research groups.[22-26] It was reported that the Tafel slope similar to our results was consistent with CO_2 reduction mechanism through the transfer of one electron to CO_2 adsorbed on the electrode surface as an initial RDS.

In summary, the long-term electrocatalytic stability of Sn nanoparticles for gaseous CO_2 reduction was extended in a zero gap electrolytic cell. Further investigations on enhancing the efficient CO_2 conversion into HCOOH are underway in conjunction with optimizing electrolyzer's conditions such as reactor design, stacking technology and modifying electrode configuration relative to the activation of RDS.

Conclusions

A direct zero-gap electrolytic cell was successfully used for the electrochemical reduction of gas-phase CO_2. We fabricated a gas diffusion electrode with placed Sn nanostructure on carbon for the stable production of HCOOH. A Tafel plot showed that the reduction mechanism is dominated by the formation of CO_2 radical anion adsorbed on the electrode surface. The direct supply of gas-phase CO_2 could aid the development of advanced industrial processes. Sustainable energy sources such as solar, wind, and geothermal electricity could be used as a continuous power source in order to decrease the overall cost for CO_2 utilization.

Acknowledgements

This work is supported by the Core Technology Development Program of the Research Institute for Solar and Sustainable Energies (RISE), Gwangju Institute of Science and Technology.

Experimental Section

Fabrication method of MEA

The fabrication of membrane electrode assembly (MEA) was simplified and effectively carried out by loading Sn nanopowder (Sigma-Aldrich, > 99%, an average particle size of 100 nm, 3.5 mg cm^{-2}) as a cathode catalyst onto the carbon diffusion paper with 30wt.% of catalyst of Nafion solution (Sigma-Aldrich, 10%) using a spray method.[13,26] This hydrophobic cathode electrode could enhance the humidity of CO_2 gas supplying networks compared to the hydrogen evolution reaction (HER) in the liquid and more favorable for liquid products discharge from the GDE. Pt/C (Johnson Matthey, 40%, 0.3 mg cm^{-2}) anode was prepared in the same manner as that of cathode. The electrodes were placed on both sides of a proton exchange solid polymer electrolyte membrane (Nafion 115, Dupont). The assembly of 9 cm^2 active area was hot-pressed at a temperature of 140°C and a pressure of 3 MPa for 5 min.

Experimental set-up for gas-phase CO_2 electroreduction

The electroreduction of CO_2 was carried out in a zero gap cell operated by electrochemical workstation (Figure S2). A potentiostat (PGSTAT-302N, Autolab) was used to apply a cathodic voltage of -0.7 V (vs. RHE). The MEA was activated with H_2 (20 ml min^{-1}) at the anode and CO_2 (40 ml min^{-1}) with 100% relative humidity at the cathode. Linear sweep voltammetry (LSV) was performed at a scan rate of 20 mV s^{-1} for testing electrocatalytic activity and a Tafel plot of CO_2 reduction was extracted to obtain information about the reaction mechanism.

Products and electrodes analysis methods

To quantify the concentration of produced HCOOH, UV-spectroscopy (UV-1800, Shimadzu) was employed for analyzing liquid phase samples (Figure S3). High performance liquid chromatography (HPLC) (Alliance 2690, Waters) with Shodex RSpak KC-G and KC-811 column was also utilized to evaluate the liquid phase product. 3 mM perchloric acid ($HClO_4$) was selected as a mobile phase with a flow rate of 1 ml min^{-1} at 25°C. HPLC analysis showed that the HCOOH peak at the retention time of 9.19 min was the sole liquid product from electrochemical CO_2 reduction (Figure S4). On the other hand, the gas-phased reaction product was detected by gas chromatography (GC) (Agilent 7890A, Agilent Technologies) equipped with thermal conductivity detector (TCD). Carboxen 1006 PLOT column (Superico) was used with the carrier gas of N_2 flowed at 1.5 ml min^{-1} (Figrue S3). In addition, the carbon source for the formation of HCOOH was identified through 1H-nuclear magnetic resonance (NMR) (Varian Inova-600 MHz, Varian) spectroscopy analysis at Korea Basic Science Institute (KBSI, Gwangju Center, Korea). $^{13}CO_2$ gas (99 atom% ^{13}C, Sigma Aldrich) was utilized to reveal the reactive origin of carbon. The morphology and phase of the crystallites of Sn nanopowders on the electrode were examined by field scanning electron microscope (FE-SEM, S-4700, Hitachi) and X-ray diffraction (XRD, Miniflex II, Rigacku), respectively.

Notes and references

1. M. E. Boot-Handford, J. C. Abanades, E. J. Anthony, M. J. Blunt, S. Brandani, N. M. Dowell, J. R. Fernandez, M.-C. Ferrari, R. Gross, J. P. Hallett, R. S. Haszeldine, P. Heptonstall, A. Lyngfelt, Z. Makuch, E. Mangano, R. T. J. Porter, M. Pourkashanian, G. T. Rochelle, N. Shah, J. G. Yao, and P. S. Fennell, *Energy Environ. Sci*., 2014, **7**, 130.
2. N. M. Dowell, N. Florin, A. Buchard, J. Hallett, A. Galindo, G. Jackson, C. S. Adjiman, C. K. Williams, N. Shah, and P. Fennell, *Energy Environ. Sci.*, 2010, **3**, 1645.
3. D. M. Attanasio, *The Environmental Law Reporter*, 2009, **39**, 10376.
4. G. Centi, E. A. Quadrelli and S. Perathoner, *Energy Environ. Sci.*, 2013, **6**, 1711.
5. J. Lee, Y. Kwan, R. L. Machunda, H. J. Lee, *Chem. Asian J.*, 2009, **4**, 1516.
6. M. Azuma, K. Hashimoto, M. Hiramoto, M. Watanabe, T. Sakata, *J. Electrochem. Soc.*, 1990, **137**, 1772.
7. Y. Hori, in Modern Aspects of Electrochemisty, ed. C. G. Vayeanas, R. White and M. E. Gamboa-Aldeco, Springer, New York, 2008, No. 42. pp. 141-153.
8. M. Jitaru, D. A. Lowy, M. Toma, B. C. Toma, L. Oniciu, *J. Appl. Electrochem.*, 1997, **27**, 875.
9. Det Norske Veritas (DNV), Electrochemical Conversion of CO_2 – Opportunities and Challenge, Norway, 2011, pp.7-8
10. R. P. S. Chaplin and A. A. Wragg, *J. Appl. Electrchem.*, 2003, **33**, 1107.
11. D. T. Whipple and P. J. A. Kenis, *J. Phy. Chem. Lett.*, 2010, **1**, 3451.
12. D. Preti, C. Resta, S. Squarcialupi and G. Fachinet, *Angew. Chem. Int. Ed. Engl.*, 2011, **123**, 12759.
13. P. Yan, F. Jin, J. Cao, B. Wu and G. Zhang, *AIP Conf. Proc.*, 2010, **1251**, 242.
14. R. L. Machunda, H. Ju, J. Lee, *Curr. Appl. Phys.*, 2011, **11**, 986.
15. R. L. Machunda, J. Lee, J. Lee, *Surf. Interface Anal.*, 2010, **42**, 564.
16. L. M. Chiacchiarelli, Y. Zhai, G. S. Frankel, A. S. Agarwal, N. Sridhar, *J. Appl. Electrchem.*, 2012, **159**, F353.
17. I. Berregi, G. D. Campo, R. Caracena, J. I. Miranda, *Talanta*, 2007, **72**, 1049.
18. P. Pullanikat, J. H. Lee, K. S. Yoo, K. W. Jung, *Tetrahedron Lett.*, 2013, **54**, 4463.
19. S. S. Asl, D. D. Macdonald, *J. Electrochem. Soc.*, 2013, **160**, H382.
20. M. Jitaru, *J. Chem. Technol. Metall.*, 2007, **42**, 333.
21. H. Li and C. Oloman, *J. Appl. Electrochem.*, 2005, **35**, 955.
22. N. F. Bunkin, P. S. Ignatiev, V. A. Kozlov, A. V. Shkirin, S. D. Zakharov and A. A. Zinchenko, *Water*, 2013, **4**, 129.

23. Y. H. Chen and M. W. Kanan, *J. Am. Chem. Soc.*, 2012, **134**, 1986.
24 A. Katoh, H. Uchida, M. Shibata and M. Watanabe, *J. Electrochem. Soc.*, 1994, **8**, 2054.
25. J. Ryu, T. N. Andersen and H. Eyring, *J. Phys. Chem.*, 1972, **76**, 3278.
26. P. G. Russel, N. Kovac, S. Srinivasan and M. Steinberg, *J. Electrochem. Soc.*, 1977, **38**, 1329.
27. A. Bandi, *J. Electrochem. Soc.*, 1990, **137**, 2157.